

Supporting Information online

**THE RIVER BLINDNESS DRUG IVERMECTIN
AND RELATED MACROCYCLIC LACTONES INHIBIT
WNT-TCF PATHWAY RESPONSES IN HUMAN CANCER**

Alice Melotti*, Christophe Mas*, Monika Kuciak*, Aiala Lorente-Trigos,
Isabel Borges and Ariel Ruiz i Altaba*

University of Geneva, Dept. of Genetic Medicine and Development,
8242 CMU, 1 rue Michel Servet, CH-1211 Geneva, Switzerland

•equal first authorship

*To whom correspondence should be addressed: +41-22-379-5646

Ariel.RuizAltaba@unige.ch

Supporting Figures

Figure S1. Luciferase assays of the top 9 hits.

Representative Luciferase reporter assays in 293T cells performed in triplicates with the top 9 antagonist candidates, confirming the results of the screen. Histogram shows averages with error bars representing s.e.m.

Figure S2. Gene expression and anti-proliferative effects of top hit 4B5 in various colon cancer cells.

A) Histogram of percentage changes of experimental gene expression over DMSO control for the genes shown after normalization by housekeeping gene levels in Ls174T and primary human colon cancer CC14 cells with 4B5 at 10 μ M 12h post-treatment. Actual values are indicated above the columns. All changes are significant over controls (T-test $p < 0.05$).

B) Histogram of the quantification of the effects of different concentrations of compound 4B5 on BrdU incorporation in the human colon cancer cell line Ls174T and the primary human colon cancer CC14 and metastatic mCC11 cells. Values are percentage incorporation equating the levels of control DMSO-treated cells to 100%. Asterisks denote significant changes over control (T-test $p < 0.05$)

Error bars = s.e.m.

Figure S3. Structures and activities of selected macrocyclic lactones.

A,D) Name, composition and chemical structure of macrocyclic lactones. Note mixtures are denoted by the varying R group. Major changes in structures are highlighted with red circles.

B,C,E) Tables of percentage BrdU incorporation shown as averages of triplicates normalized over DMSO controls (equated to 100%) over a range of concentrations. Calculated IC₅₀'s with PRISM are given in the rightmost columns. StromectolTM is a commercial name of oral Ivermectin used. Results are shown for multiple human cancer types (B,C) and multiple human colon cancer cells (E).

Figure S4. Ivermectin and Selamectin inhibit colon cancer stem cell self-renewal during clonogenic assays.

Histogram of the percentage of spheroid formation in each condition as indicated. Treatment with DMSO (as control) or with Ivermectin at 1 μ M or 5 μ M started at the time of clonal plating for spheroid formation.

Error bars = s.e.m. Probability (p) values are derived from 2-tailed T-tests. No p values are possible for comparison with zero values at 5 μ M.

Figure S5. Inhibitory effects of Stromectol™ and Ivermectin on DLD1 and H358 xenografts, respectively.

A) Graph of tumor growth in control or Stromectol-treated mice bearing DLD1 xenografts. See Figure 3A for comparison with Ivermectin. In all cases treatment began after tumor establishment. Stromectol™ pills from the local pharmacy were grounded and the powder dissolved in DMSO, then mixed with cyclodextrin as with Ivermectin, aiming at a similar dose (10mg/kg/daily) as given with Ivermectin conjugated with cyclodextrin. We note that the exact amount of active ingredient is likely to vary.

B) Inhibitory effects of Ivermectin on the growth of human metastatic bronchialveolar carcinoma H358 xenografts.

C) Left panel) Heat map of gene expression shown as ratios determined by rt-qPCR of experimental over controls after normalization with housekeeping genes, revealing the repression of WNT-TCF targets by Ivermectin in H358 cells. Right panel) Western blots showing the repression of CYCLIN D1 protein levels by Ivermectin treatment in H358 cells. Control GAPDH levels are shown for each condition.

Error bars = s.e.m. Probability (p) values are derived from 2-tailed T-tests.

Figure S6. Diagram of direct activation of TCF by the fusion protein TCF^{VP16} and IC50 curves for treated Ls174T cells.

A) Diagram of the suggested action of macrocyclic lactones on β -CATENIN-TCF-driven transcription of targets and its rescue by the function of a TCF-VP16 transactivating domain fusion that acts as a dominant-active TCF independent of β -CATENIN.

B) IC50 curves of BrdU incorporation for Ivermectin (left) or Selamectin (right) treatments with primary human colon cancer CC36 cells. In each graph there is the superimposition of the response of control (empty vector) and TCF^{VP16} expressing cells to different drug concentrations. Blue arrows show the shift in IC50 values. Error bars = s.e.m. See Figure 5A.

Figure S7. Repression of C-terminal phosphoforms of β -CATENIN and CYCLIN D1 by Ivermectin in Ls174T cells.

Western blots of Ls174T human colon cancer cell extracts showing the concentration-dependent loss of C-terminal phosphoforms of β -CATENIN (P-ser552 and P-ser675) and CYCLIN D1 by treatments with Ivermectin. See Figure 6. GAPDH and total β -CATENIN levels are shown as controls.

Figure S8. Okadaic acid effects and rescue of Ivermectin repression of C-terminal phosphoforms of β -CATENIN and CYCLIN D1.

A) Dose-dependent increases of C-terminal phosphoforms of β -CATENIN and of the levels of CYCLIN D1 in DLD1 cells treated with Okadaic acid (OA).

B) Western blots of DLD1 cell extracts showing varying levels of C'-phosphoforms of β -CATENIN and of CYCLIN D1 treated with (+) 15nM Okadaic acid (OA) as compared with DMSO only (-) controls. Treatment with OA, which represses the activity of the protein phosphatases PP2A and PP1, rescues the repression of these proteins by Ivermectin treatment (2.5 μ M and 5 μ M, gray triangle). The control and experimental lanes are from the same Western blot (see Source data for FigS8B).

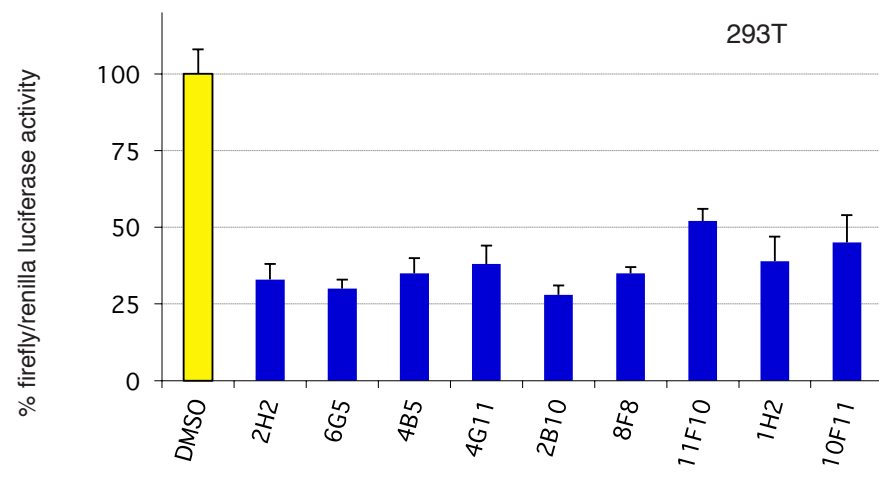
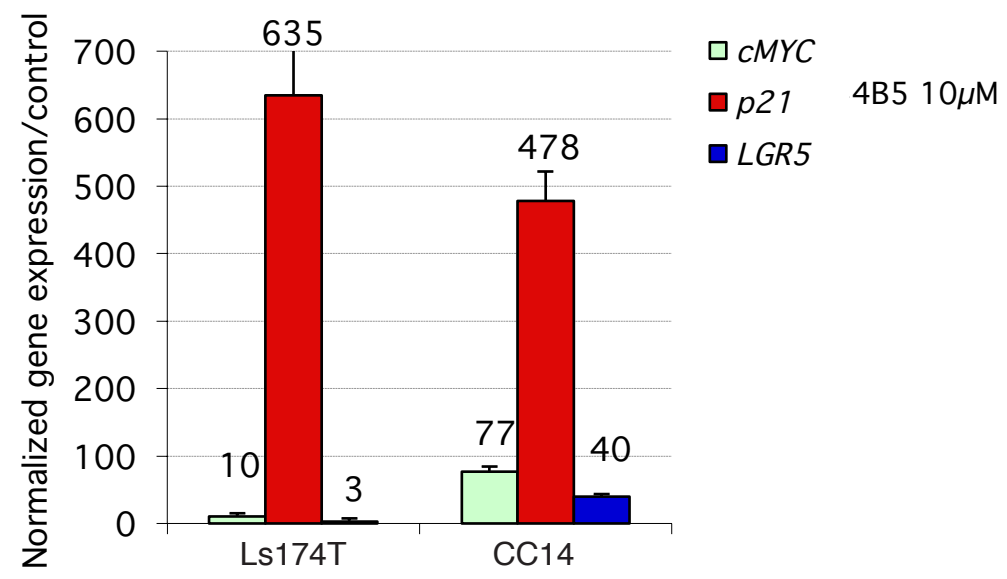


Fig S1

A



B

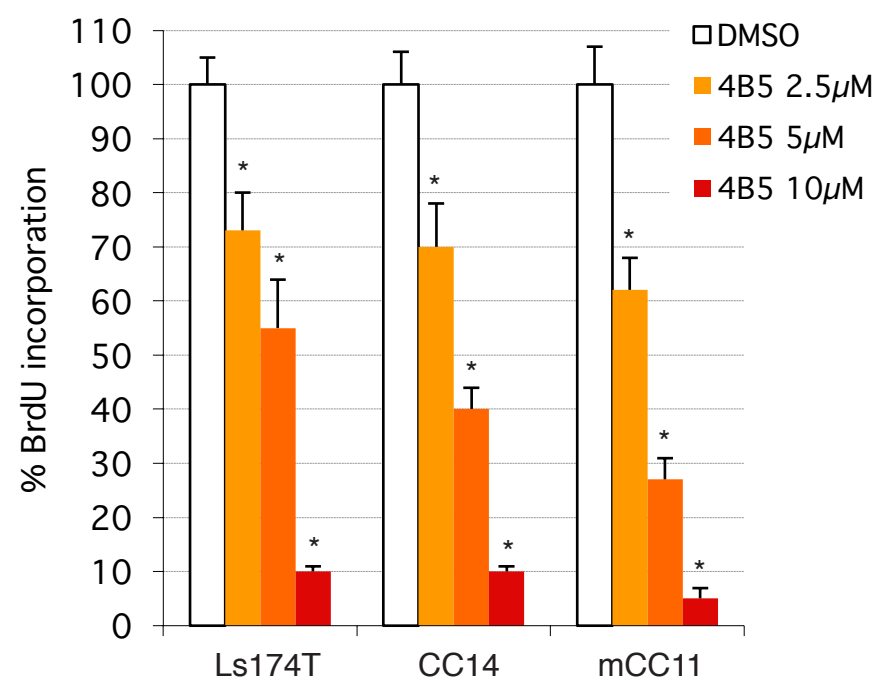


Fig. S2

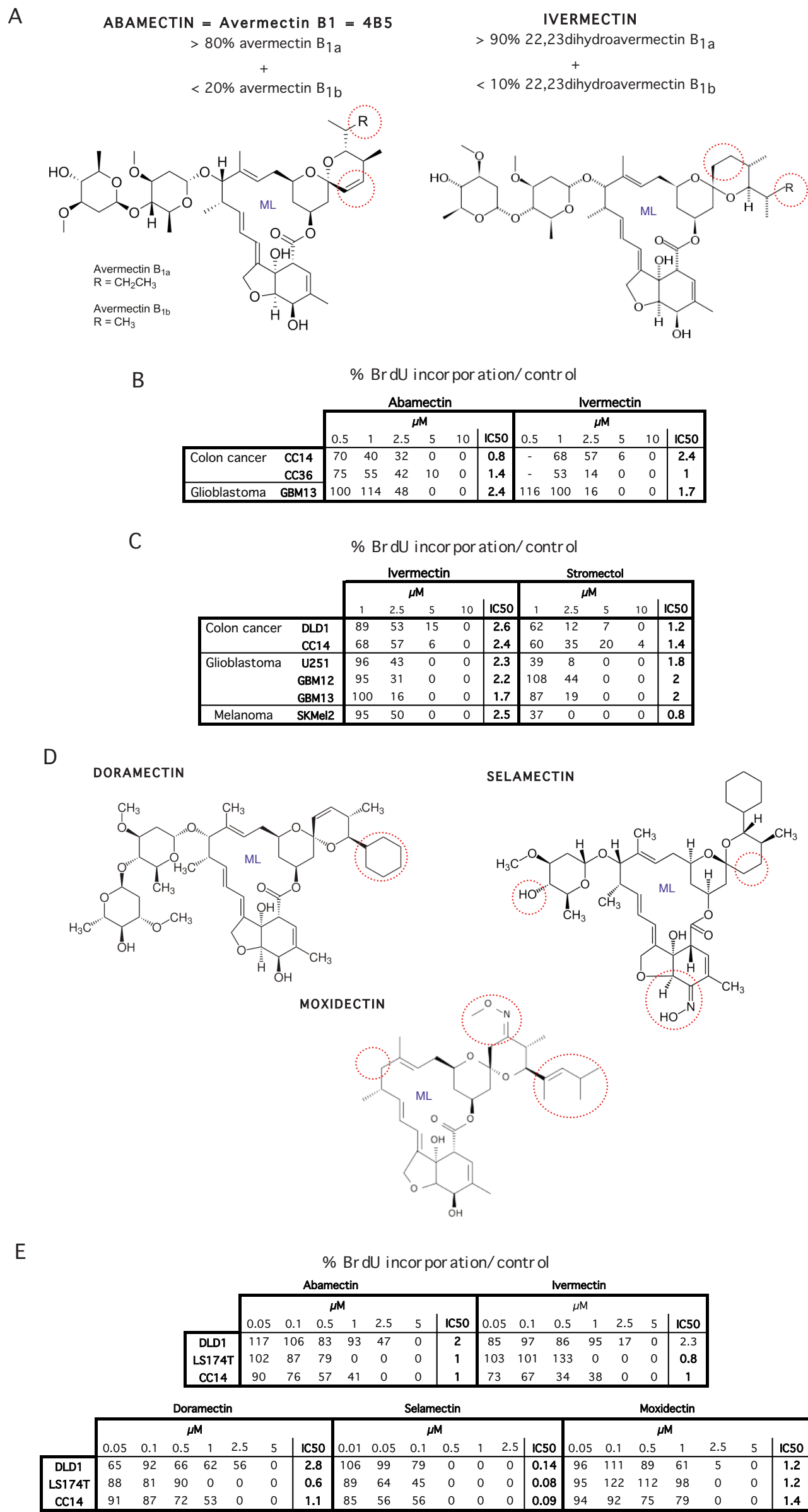


Fig. S3

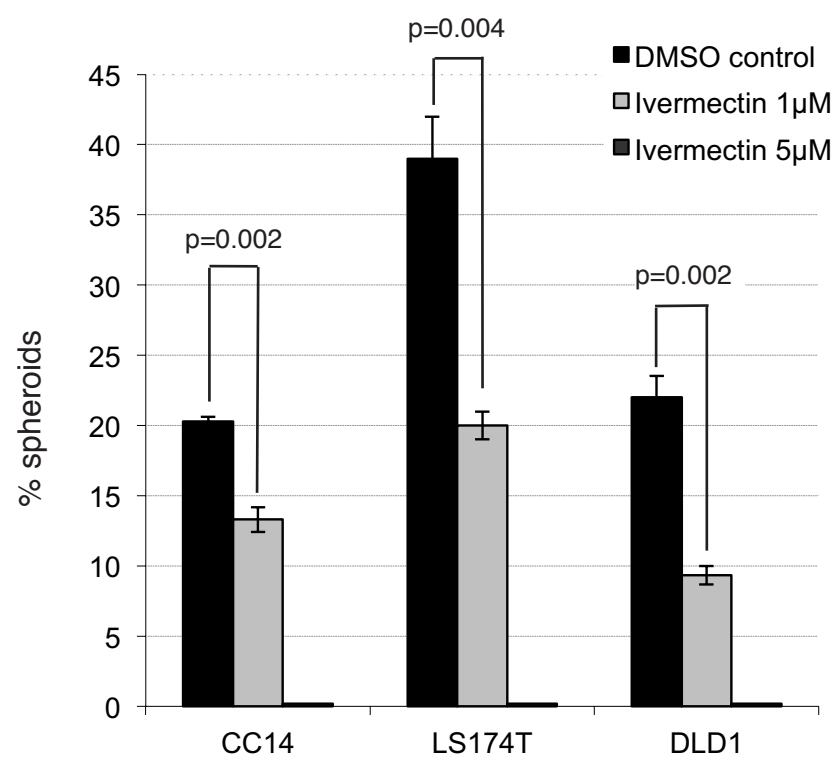
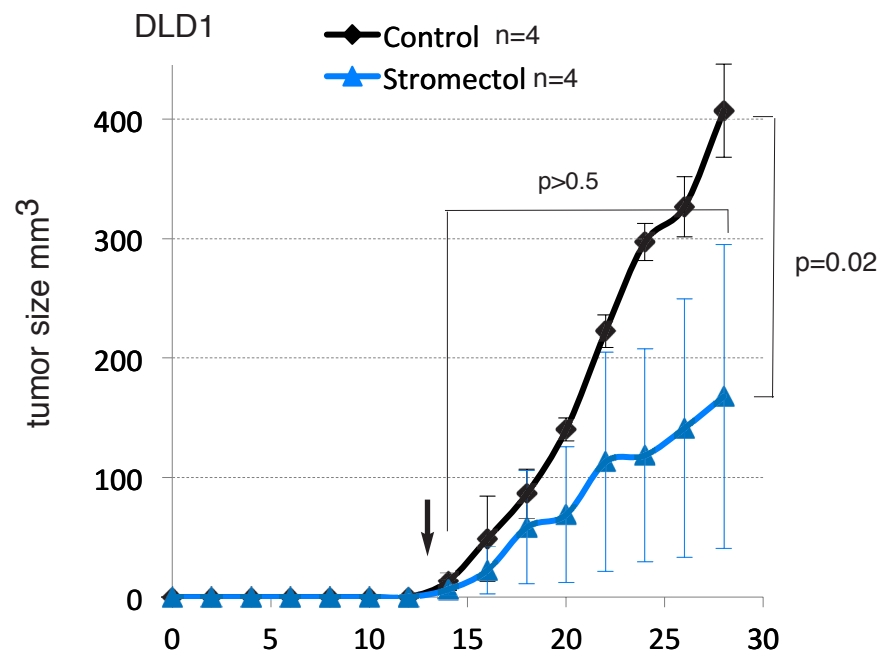
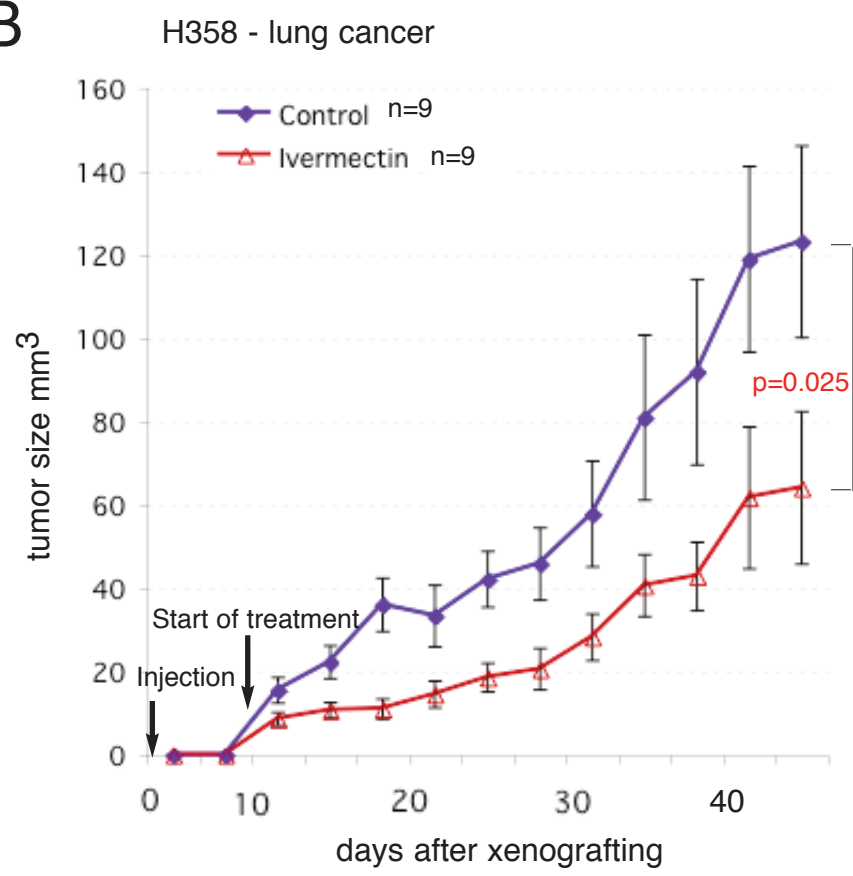


Fig. S4

A



B



C

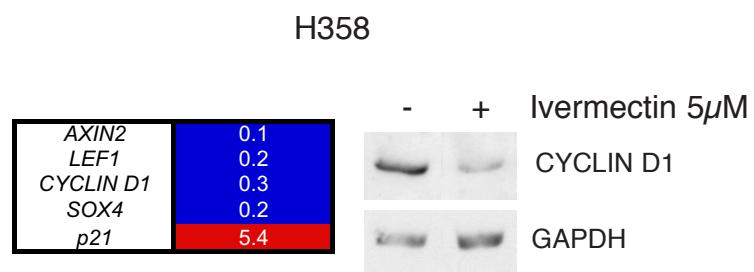


Fig. S5

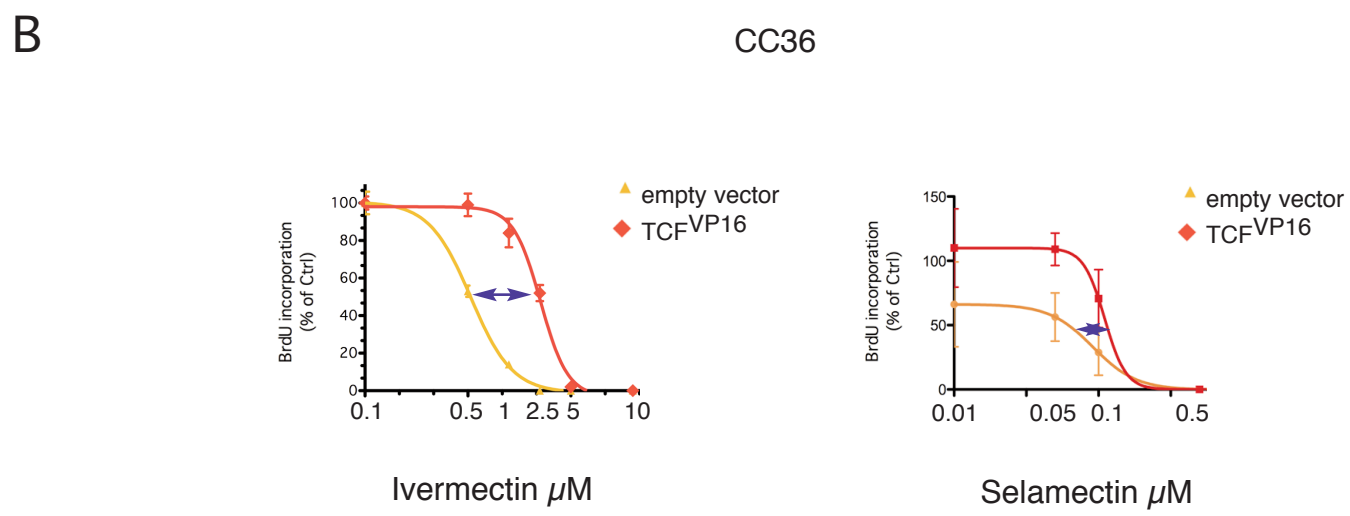
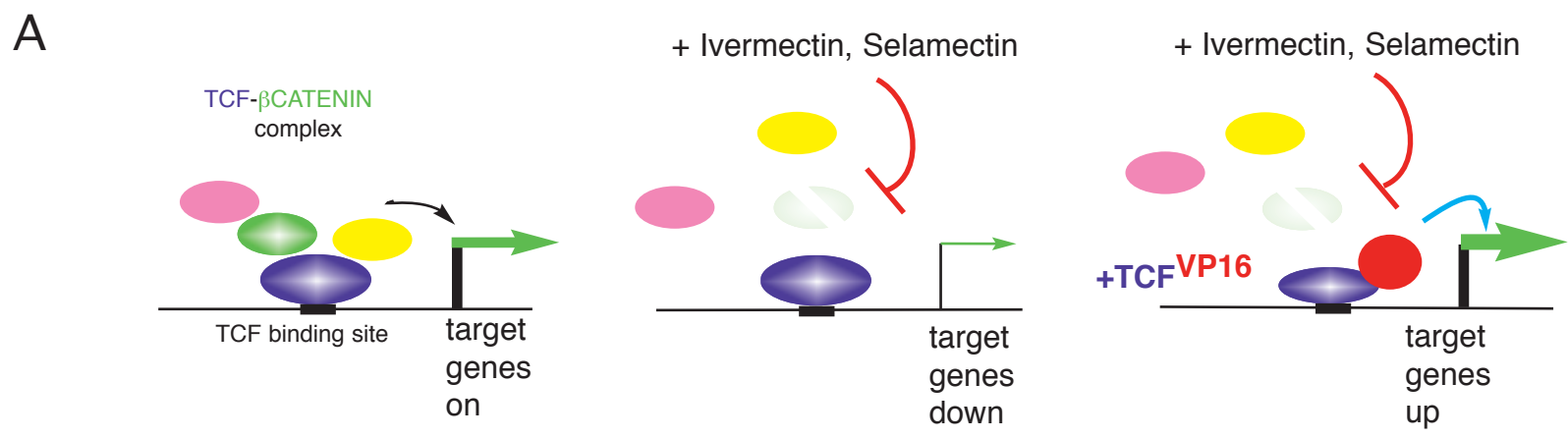


Fig. S6

Ls174T

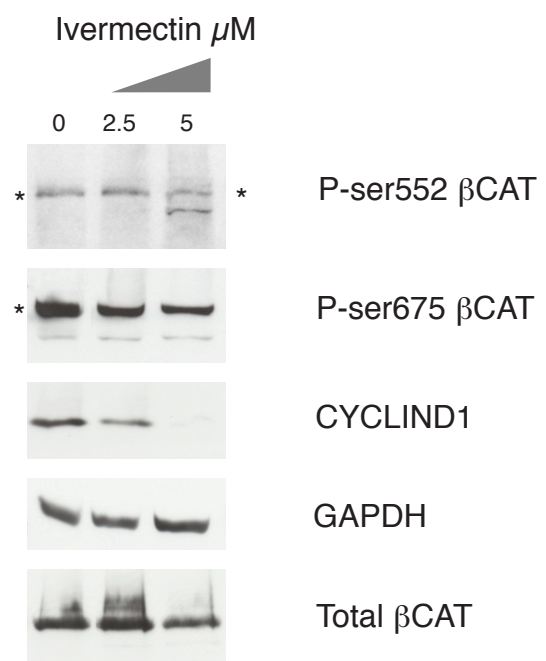
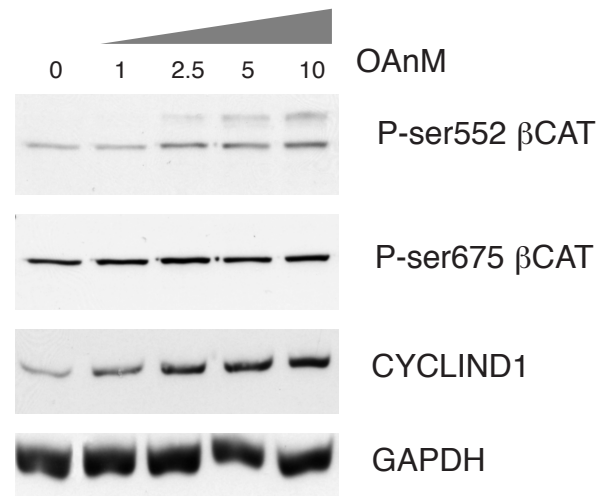


Fig S7

A



B

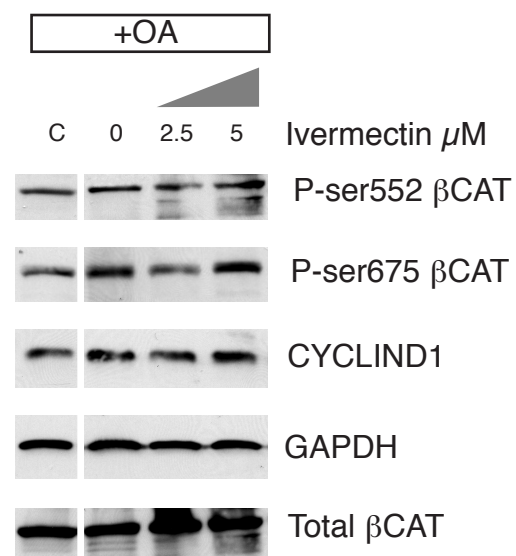


Figure S8